ACS Macro Letters

Letter

pubs.acs.org/macroletters

# Dispersing Grafted Nanoparticle Assemblies into Polymer Melts through Flow Fields

Joseph Moll,[†] Sanat K. Kumar,[*,‡] Frank Snijkers,[§,∥] Dimitris Vlassopoulos,[*,§,∥] Atri Rungta,[⊥] Brian C. Benicewicz,[⊥] Enrique Gomez,[#] Jan Ilavsky,[○] and Ralph H. Colby[△]

[†]Department of Chemistry, Columbia University, 5000 Broadway, New York, New York 10027, United States

[‡]Department of Chemical Engineering, Columbia University, 500 West 120th Street, New York, New York 10027, United States

[§]Institute of Electronic Structure and Laser, Foundation for Research and Technology Hellas (FORTH), P.O. Box 1527,GR-711 10 Heraklion, Greece

[∥]Department of Materials Science and Technology, University of Crete, P.O. Box 2208, GR-710 03 Heraklion, Greece

[⊥]Department of Chemistry and Biochemistry, University of South Carolina, Columbia, South Carolina 29208, United States

Departments of [#]Chemical Engineering and [△]Material Science and Engineering, Pennsylvania State University, University Park, Pennsylvania 16802, United States

[○]X-ray Science Division, Advanced Photon Source, Argonne National Laboratory, Argonne, Illinois 60439, United States

Supporting Information

**ABSTRACT:** Flow-fields are typically used to intimately mix large $\mu$m-sized particles with polymer melts. Here we show, using rheology, X-ray scattering, and electron microscopy, that shear flows do not improve the spatial dispersion or ordering of spherical nanoparticles (NP) grafted with polymer chains over the ranges of flow fields realizable in our experiments in the melt state. In the absence of flow, grafted NPs robustly self-assemble into a variety of superstructures when they are added to a homopolymer matrix with the same chemistry as the NP grafts. We find that isolated particles and spherical NP clusters remain dispersed but do not flow align. On the other hand, anisotropic NP assemblies initially break and their constituent building blocks (strings or sheets) flow-align locally. At very large strains, they coarsen into large aggregates, reflecting the dominance of interparticle attractions over flow fields and thermal energy.

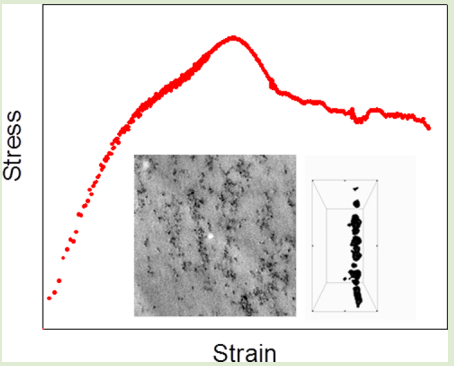


Nanosized, inorganic fillers are of interest because they can significantly enhance the mechanical,[1−4] electrical,[2,5] optical, and gas permeability[6] properties of the polymers to which they are added. Past work has demonstrated the crucial importance of NP dispersion state in this context.[7−11] It has been shown that some material properties are optimized when the NPs are randomly dispersed,[12] while others require the NPs to align in a given direction[13,14] or form percolated structures.[9,11] We have outlined a robust self-assembly method to achieve some of these goals in the quiescent state, that is, in the absence of flow.[15−19] Specifically, we considered NPs grafted with polymer chains, in the case where the particle cores and grafted chains repel. These hairy NPs behave akin to amphiphiles and self-assemble into a variety of morphologies, depending on graft length and density even when they are dispersed in a homopolymer with the same chemical structure as the grafts (Figure 1). When the NPs are densely grafted with long chains, they are well dispersed in a polymer matrix due to steric stabilization, that is, NP−NP attraction is strongly reduced by the presence of the grafted chains. In the opposite limit of sparse grafting of short chains, the NPs and matrix phase separate, creating spherical NP clusters, reflecting a dominance of NP−NP attractions. Intermediate values of grafting density and length yield a variety of anisotropic interconnected structures such as NP strings and NP sheets (Figure 1), due to a balance of NP−NP attractions and the steric stabilization of the brush which leads to patchy (anisotropic) interactions.[20,21] It is thus important to have a good estimate of the (bare) inter-NP attraction, $U$, relative to the thermal energy $kT$, and simulations[20] yield $\zeta = U/kT \sim 10$, comparable to attractive colloidal systems, for example, gels.[22−24]

In this paper we critically examine the use of achievable shear flow fields (and extensional flows in a few limited cases) to control and potentially improve the spatial dispersion of NPs. We show that anisotropic NP assemblies (consisting of polystyrene-grafted silica particles in polystyrene matrix) can both break and locally orient in shear. While these assemblies break into smaller structures, they do not go all the way back to the building blocks, that is, individual NPs, for the flow rates we

**Received:** August 29, 2013
**Accepted:** October 31, 2013

   dx.doi.org/10.1021/mz400447k | *ACS Macro Lett.* 2013, 2, 1051−1055

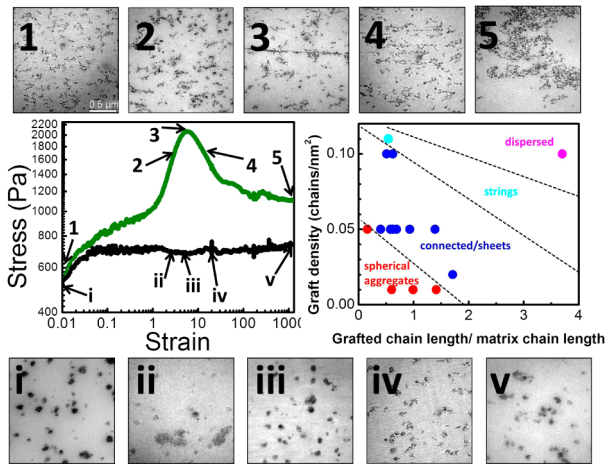


**Figure 1.** Left plot shows stress−strain curves for two samples with different quiescent dispersion states from step-rate experiments (180 °C, shear rate 0.1 $s^{-1}$): Interconnected initial dispersion state (green) and small roughly spherical particle aggregates (black). The TEMs show the evolution of the morphology diagram in these samples at strains of 0 (1, i), 3 (2, ii), 8 (3, iii), 14 (4, iv), and 1200 (5, v), respectively: the top sequence corresponds to NP strings (initially), while the bottom row corresponds to spherical agglomerates. All images are oriented such that the flow and gradient directions are the horizontal and vertical directions, respectively. The right plot shows an experimental "morphology diagram" of the polymer-tethered particles mixed with matrix polymers.[15] The different regions represent different particle dispersion states. The red region represents spherical aggregates, the blue region represents sheets and interconnected structures, the cyan region represents short strings and the magenta region represents dispersed particles. The lines that separate different regions are merely guides to the eye. All samples included in the plot are listed in Table S1.

achieve in our setups. In the case of spherical structures, for example, individual NPs or spherical clusters, no flow induced changes are found for the same amount of applied shear.

Before studying NPs, it is instructive to consider non-interacting large colloidal particles suspended in viscoelastic matrices, for which the primary effects of shear are accounted for by the particle and matrix time scales via the Peclet and Weissenberg numbers, $Pe = \tau_{particle}\dot{\gamma} = 6\pi\eta\dot{\gamma}R^3/kT$ and $Wi = \tau_{polymer}\dot{\gamma} = \eta\dot{\gamma}/G_e$, respectively. For typical size $R \sim 1$ $\mu$m colloids imaged in optical microscopy, with matrix zero-shear viscosity $\eta = 100$ Pa·s, matrix plateau modulus $G_e \approx 10^2$ Pa and shear rate $\dot{\gamma} = 1$ $s^{-1}$ we get $Pe \sim O(10^5)$ and $Wi \sim O(1)$, meaning that large colloidal particles diffuse much more slowly than polymer chains. This yields flow-alignment of the particles, namely, the flow can alter the particle dispersion state, while affecting the surrounding matrix to a lesser degree.[25−29] The NPs at hand are much smaller with $R = 7$ nm, suspended in a matrix with $\eta = 10^4$ Pa·s and $G_e \approx 10^5$ Pa. Thus, $Pe \sim O(10)$ and $Wi \sim O(10^{-1})$ for the same shear rate. Consequently, the shear time is not significantly smaller than the NP self-diffusion time. Additionally, $Pe/\zeta = 6\pi\eta\dot{\gamma}R^3/U \sim O(1)$, that is, the viscous drag is comparable to the NP−NP bonding. These arguments suggest that the key dimensionless material parameters involved in the shearing process, that is, particle relaxation time (Pe), NP−NP attractions ($\zeta$), and matrix relaxation time (Wi) are all roughly comparable, implying that flow-induced NP ordering is a subtle issue.

RAFT polymerization is used to grow polystyrene chains of various lengths and densities from 14 nm silica particles.[18] The grafted particles are dissolved in tetrahydrofuran (THF) and monodisperse polystyrene is added to this mixture. The samples, containing 5 wt % of the silica core, are mixed in a vortex, and then by pulsed sonication; they are then solvent-cast, dried overnight in a vacuum, and annealed for 5 days at 150 °C. Transmission electron microscopy (TEM), ultra-small-angle X-ray scattering (USAXS), and rheology are used to analyze the samples while recording their orientation relative to the flow direction. All rheology measurements are conducted at 180 °C with an ARES 2kFRTN1 strain-controlled rheometer. To avoid edge fracture and wall slip problems as a source of rheological artifacts, a cone (0.1 rad angle) and plate geometry (8 mm diameter) with a partitioned ring (CPP) forming a gap of 0.15 mm, is used in most rheological tests. This geometry (with an accompanying extension of the ARES oven) was custom built,[30] based on a system first proposed by Meissner et al.[31,32] We note, however, that despite the quantitative rheological implications, no major morphological differences were observed by TEM when samples were sheared in cone and plate, CPP, or parallel plate geometries (Supporting Information, Figure S1). Each sample was split into eight, and independent flow experiments were performed on each one. Each sample was taken to a different final strain and then quenched to room temperature. The quenched samples were observed using TEM and image analysis was averaged over 100 micrographs. The microtomed sections were taken 1 mm into the 8 mm diameter disc. For strain recovery experiments, a Physica MCR-501 stress-controlled rheometer (Anton Paar, Austria) was used with the above cone and plate setup but without CPP.

We report here on start-up of steady shear (step-rate) experiments at 180 °C, that is, 80 °C above the glass transition temperature ($T_g$) of polystyrene. Start-up of steady shear experiments were performed on two different dispersion states, one in which the NPs form small spherical aggregates (of typical size 150 nm), and the other where the particles assemble into anisotropic structures, that is, small sheets, of thickness of the order of the particle size. To determine the structural origins of the qualitatively different stress responses, we used TEM and verified the conclusions using USAXS[33,34] (see Supporting Information, Figure S2). Strains on both sides of the stress maximum (near strain = 8, see Figure 1) were studied, namely 0, 1, 3, 8, 14, 59, 400, and 1200. The same strains were used for the spherically aggregated sample, which however did not show a stress maximum.

The rheology results show important differences in stress/strain curves for the different NP dispersion states studied. We first consider a nanocomposite comprised of spherical NP clusters, which displays effectively no stress overshoot, and shows hardly any changes in aggregation state on shearing (Figure 1). While there may be sample-to-sample variations in the individual TEMs, the calculated radially averaged correlation function (which is obtained from 100 such TEM images for each strain), remains practically invariant with applied strain (Supporting Information, Figure S3b). Next, we focus on an initially aggregated state, with self-assembled particle sheets of sizes 14 nm (thickness) × 140 nm (length) × 100 nm (width). Figure 1 shows a complex stress response with a pronounced overshoot (green data) at the strain rate of 0.1 $s^{-1}$. We note that from the low-strain linear stress response a constant slope (i.e., modulus) of about $10^5$ Pa is extracted. This is remarkably close to the plateau modulus of the polystyrene matrix, suggesting that the initial stress response is dominated


dx.doi.org/10.1021/mz400447k | ACS Macro Lett. 2013, 2, 1051−1055

by the fastest relaxing component, the polymer. The onset of nonlinear response, at a strain of about 0.02, represents a crossover to the NP-assembly response. We previously found that stress overshoots are typically only seen when the NPs form "assembled" structures such as sheets, strings or interconnected structures.[7,9] Rheology experiments suggest that, at these loadings, the NPs are "connected" on average to two other particles.[35] While we expect that these NP "bonds" break beyond a strain of 0.02,[36,37] elastic deformation still appears to control this regime. Experimental evidence for this conclusion comes from the fact that when the stress was removed at different strains between the first kink and the overshoot (which we assign to the second, main yield point at a strain of 8), the recovered compliance was very high. This suggests that even though individual bonds may break, the whole NP-assembly deforms significantly before yielding occurs (Supporting Information, Figure S4 for a particle loading of 15%). The progressive stretching of the structures increases the stress, and at the same time some of the broken anisotropic building blocks orient locally (see TEM image 2, Figure 1). Note that the main yield strain of ~8, which is very large compared to typical colloidal gels,[36] is consistent with the notion that there is very small loading of NPs; thus, the structure that forms is very open and, therefore, deformable.[38]

In the vicinity of the stress peak, that is, the main yield point, the structures are broken into pieces of various sizes and maximum orientation is observed. Indeed, while many small particle sheets appear dispersed in the matrix at this concentration, a few of them appear to aggregate into a single layer, forming an oriented structure (Figure 1, TEM image 3; TEM tomography results, Figure 2). Substantiation for this

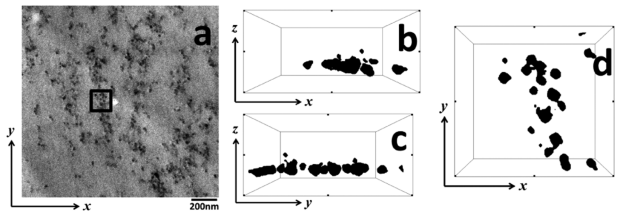


**Figure 2.** Tomographical images of the sample with interconnected structures in Figure 1 after shearing at 180 °C to a strain = 8 (where maximum alignment is seen). (a) TEM image. (b–d) The sample in the *xy*, *xz*, and *yz* planes, respectively, where *x* is the vorticity direction, *y* is the flow direction, and *z* is the gradient direction.

conclusion comes from ultra-small-angle X-ray scattering results that clearly show alignment when the sample is viewed from an edge on view (Supporting Information, Figure S2b). Here the scattering is clearly anisotropic, with a characteristic length scale that nearly triples on the application of shear (from ~70 to ~180 nm). Apparently, flow aligns the domains along its direction, but in such a way that "layers" are created along the gradient direction; the mean "separation" between layers in the gradient direction increases on the application of flow, explaining the larger ~180 nm length scale that emerges. This is consistent with sheets of particles, which orient in the direction of flow, such that when a cross section is viewed from the edge they appear as aligned strings, but when viewed from the top they appear as small clusters of particles with minimal alignment. Similar results were obtained for the string state, implying that these trends persist for all the anisotropic NP assemblies that we have examined (Supporting Information, Figure S5).

As for the decrease of the stress beyond the peak to steady state with continuous shearing, this results from coarsening of the broken pieces[39−43] with large areas of solvent matrix (heterogeneity, Figure 1, TEM image 4). The coarsening is attributed to flow-induced diffusion and presumably the "phase separation" that occurs at these large deformations. Interestingly, this phenomenon does not significantly affect the steady stress value, probably because of the low NP loading. The percolated polymer phase thus dominates the shear response. The above points are also well-illustrated in the radially averaged NP−NP correlation function in the flow-gradient plane (Supporting Information, Figure S3a). There is no change in this function until after the stress maximum, but a steady change afterward. These results are apparent even from a visual analysis of the TEM (Figure 1).

Our previous work[44] has shown that, in the initial states, these self-assembled morphologies are frequently temporally evolving, implying directional phase separation. Similarly, the steady-state morphologies are metastable under shear, because these structures seem to evolve after the cessation of flow. Whereas stress relaxation upon flow cessation has been followed rheologically (Figure 3 below), the morphological

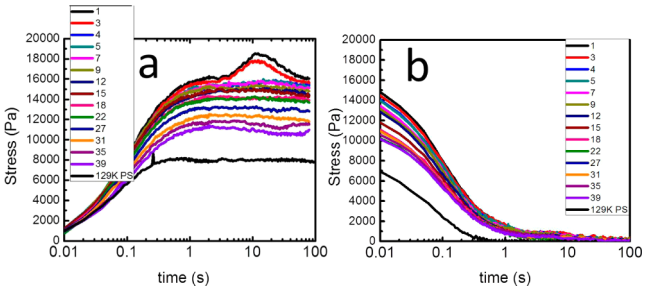


**Figure 3.** Consecutive step rate tests: Start-up of shear at a constant rate of 1 $s^{-1}$ (a) at 180 °C and stress relaxation after steady shear (flow cessation, b) for 14 nm silica with 88 K grafts with 0.05 chains/$nm^2$ in a $M$ = 129 K matrix, in the connected sheets regime of the morphology diagram (see Figure 1). Odd numbers, which are shown in the figure, correspond to clockwise rotation; even numbered experiments were in the opposite direction. The first two-step rate tests exhibit the stress maximum, while quite remarkably, subsequent step rate tests show a progressive lowering of the steady state viscosity without stress overshoot. Similarly, the stress of the NP network, seen in the cessation experiments after a waiting time ~ 5 s, progressively lowers and disappears fully after 20 repeats. Relaxation was allowed to occur for 300 s total between step rate experiments (which were taken to a strain of 80 and, thus, proceeded for 80 s).

changes will be the subject of future investigations. The important finding is that the applied flow field cannot fully disperse the NP self-assembled structures into their constituents; instead, it leads to their coarsening.

The findings on shear-induced changes bear similarities with recent works on colloidal gels from large colloidal particles dominated by attractions. In general, it has been suggested in the literature that a fine balance of interparticle enthalpic attractions and repulsive barriers, both in terms of strength and range, as well as the effects of gravity, may lead to a variety of situations, such as kinetic trapping of phase separation and pseudoequilibrium percolating systems.[22−24] Concerning the effects of flow on gel states, Masschaele and Vermant[45] suggested that the strain-induced affine yielding of 2D gels


dx.doi.org/10.1021/mz400447k | ACS Macro Lett. 2013, 2, 1051−1055

made of large particles involved a sequence of bond break-up and local orientation in flow, which eventually coarsen. The characteristic length scales involved depended on shear and the heterogeneity of the gel. By analogy, in our case, the string and connected sheet states are assemblies with anisotropic building blocks. Under shear, these assemblies deform, the interblock bonds break and the blocks align and often line-up in flow, presumably to minimize drag. More striking is the qualitative similarity of the present results with the recent work of Koumakis and Petekidis[36] on the yielding of colloidal gels. These gels were formed from large PMMA particles with polystyrene as depletant added at different volume fractions. Interestingly, the stress−strain response of the depletion gels was qualitatively similar to that of the NP assemblies, exhibiting two yield strains, the larger one being nearly shear-rate independent. (As noted earlier, these yield strain values are much lower for the colloidal analogs.) These yield points were attributed to gel-breaking occurring at different length scales, that is, bonds and clusters, which is very close in spirit to our own conjectures. Note that, for sufficiently high shear rates applied to such large-particle gels [exceeding $10^2$ $s^{-1}$, that is, Pe $\sim O(10^7)$], they can disaggregate completely into their individual constituents.[46,47] The highest Peclet numbers we can attain are much lower, rationalizing our findings.

From the above it is evident that establishing a connection between NP assemblies and colloidal gels is important, and the main point is that our systems can be viewed as weak gels. In all cases, yielding is shown to be a gradual process (with first and second yielding events), and here the anisotropic nature of the building blocks is responsible for their intermittent local orientation. The uniqueness of the present class of systems is that the assembly structure is based on very small anisotropic building blocks (i.e., NP strings or sheets) at extremely low volume fractions in a highly viscoelastic matrix (polymer melt). These open structures resist the imposed shear by (i) deforming and subsequently, (ii) gradually breaking their interblock bonds (first yielding) while still stretching the assembly, then (iii) orienting in flow and completely breaking (second yielding) (iv) coarsening to the final morphology. Hence, our NP anisotropic assemblies combine the features of sheared colloidal gels, nonspherical particle clusters and dominance of interparticle interactions.

Consecutive step-rate tests (start-up of shear at constant rate, Figure 3a) followed by stress relaxation after steady shear (flow cessation, Figure 3b) were also performed. In particular, Figure 3 considers a sample in the "connected sheets" regime of the morphology diagram (see Figure 1). The first two step-rate tests exhibit the stress maximum from breaking and locally aligning the assembled NP structure, while subsequent step rate tests show a progressive lowering of the steady state viscosity (without stress overshoot). Presumably, this occurs because the system gradually collapses the sheets to coarsened agglomerates of particles. Apparently, the long relaxation time of the assembly (much longer than the shearing time, see also Supporting Information, Figure S6) and the associated large NP attraction prohibit its reformation during the time scale of the experiments, which involve a 300s waiting time between successive steps, and hence no stress overshoot is further observed.[35] In the same vein, the progressive reduction of stress with the number of step tests may relate to the improved local alignment and coarsening, which are not relaxed in these experiments. Similarly, the stress of the NP assembly, seen in the cessation experiments at long times, progressively lowers and disappears fully after roughly 20 consecutive shearing episodes up to $\gamma = 80$ (and back). This is another unique feature of this system, attributed to the very slow structural time of the anisotropic particle assembly (Supporting Information, Figure S6).

Given the important role of the interplay of shear structure deformation and eventual break-up, a formidable challenge is optimizing the shearing conditions for most effective NP alignment. In part, this is motivated by the large body of work on the efficient alignment of ordered block copolymers during large amplitude oscillatory shear (LAOS).[48] In the case of block copolymers, the structures break during the LAOS cycle, but reform quickly enough that oscillatory shear aligns them. On the other hand, it takes too much time for NP structures to relax, so as to reach quasi-equilibrium at the time flow sets in (as judged from their linear viscoelastic response,[9,15] see also Supporting Information, Figure S6). We thus argue that the ultraslow time scales for the growth and equilibration of the NP structures preclude reordering and alignment on the time scale of a period of oscillation. Thus, LAOS does not improve the flow-alignment of NP structures but instead leads to a coarsening similar to that seen at large strains in steady shear (Supporting Information, Figure S7). Furthermore, uniaxial extension of films of NPs in the polystyrene matrix, which are organized into strings under quiescent conditions, does not improve the results from shear flow in terms of string alignment and does not disperse the NPs (Supporting Information, Figure S8). In this particular case, even if we applied a strong flow, the experimentally accessible range of Hencky strains (below 3.5) was too low (compared to a shear strain of 8 where local alignment was observed in simple shear), confirming that even with strong flows we need sufficiently large strains to induce macroscopic alignment of the NP assemblies.

## ■ ASSOCIATED CONTENT

### Ⓢ Supporting Information

We describe many additional experimental details and additional experiments that bolster the essential conclusions of our paper. This material is available free of charge via the Internet at http://pubs.acs.org.

## ■ AUTHOR INFORMATION

### Corresponding Author

*E-mail: sk2794@columbia.edu.

### Notes

The authors declare no competing financial interest.

## ■ ACKNOWLEDGMENTS

Financial support from the National Science Foundation to J.M. and S.K.K. (DMR 01106180) and the EU (Nanodirect CP-FP213948-2) to F.S. and D.V. is gratefully acknowledged. ChemMatCARS Sector 15 is principally supported by the National Science Foundation/Department of Energy under Grant No. NSF/CHE-0822838. Use of the Advanced Photon Source was supported by the U.S. Department of Energy, Office of Science, Office of Basic Energy Sciences, under Contract No. DE-AC02-06CH11357. We thank J. Mewis and R. Pasquino for many useful discussions and H. Lentzakis for assistance with the extensional rheometry.

## ■ REFERENCES

(1) Payne, A. R. *J. Appl. Polym. Sci.* **1965**, *9*, 2273−2284.

(2) Payne, A. R. *J. Appl. Polym. Sci.* **1965**, *9*, 1073−1082.
(3) Heinrich, G.; Klüppel, M. *Adv. Polym. Sci.* **2002**, *160*, 1−44.
(4) Gusev, A. A. *Macromolecules* **2006**, *39* (18), 5960−5962.
(5) Ounaies, Z.; Park, C.; Wise, K. E.; Siochi, E. J.; Harrison, J. S. *Compos. Sci. Technol.* **2003**, *63* (11), 1637−1646.
(6) Okada, A.; Usuki, A. *Macromol. Mater. Eng.* **2006**, *291* (12), 1449−1476.
(7) Akcora, P.; Kumar, S. K.; Moll, J.; Lewis, S.; Schadler, L. S.; Li, Y.; Benicewicz, B. C.; Sandy, A.; Narayanan, S.; Ilavsky, J.; Thiyagarajan, P.; Colby, R. H.; Douglas, J. F. *Macromolecules* **2009**, *43* (2), 1003−1010.
(8) Chevigny, C.; Dalmas, F.; Di Cola, E.; Gigmes, D.; Bertin, D.; Boué, F. o.; Jestin, J. *Macromolecules* **2010**, *44* (1), 122−133.
(9) Moll, J. F.; Akcora, P.; Rungta, A.; Gong, S.; Colby, R. H.; Benicewicz, B. C.; Kumar, S. K. *Macromolecules* **2011**, *44* (18), 7473−7477.
(10) Janes, D. W.; Moll, J. F.; Harton, S. E.; Durning, C. J. *Macromolecules* **2011**, *44* (12), 4920−4927.
(11) Shiomi, H.; Kobayashi, H.; Kimura, T.; Nakamura, M. *J. Mater. Sci.: Mater. Electron* **1996**, *7* (6), 437−445.
(12) Mackay, M. E.; Tuteja, A.; Duxbury, P. M.; Hawker, C. J.; Van Horn, B.; Guan, Z.; Chen, G.; Krishnan, R. S. *Science* **2006**, *311* (5768), 1740−1743.
(13) Park, C.; Robertson, R. E. *Dental Mater.* **1998**, *14* (6), 385−393.
(14) Prasse, T.; Cavaillé, J.-Y.; Bauhofer, W. *Compos. Sci. Technol.* **2003**, *63* (13), 1835−1841.
(15) Akcora, P.; Liu, H.; Kumar, S. K.; Moll, J.; Li, Y.; Benicewicz, B. C.; Schadler, L. S.; Acehan, D.; Panagiotopoulos, A. Z.; Pryamitsyn, V.; Ganesan, V.; Ilavsky, J.; Thiyagarajan, P.; Colby, R. H.; Douglas, J. F. *Nat. Mater.* **2009**, *8* (4), 354−359.
(16) Schadler, L. S.; Kumar, S. K.; Benicewicz, B. C.; Lewis, S. L.; Harton, S. E. *Mater. Res. Soc. Bull.* **2007**, *32*, 335−340.
(17) Li, C.; Benicewicz, B. C. *Macromolecules* **2005**, *38* (14), 5929−5936.
(18) Li, C.; Han, J.; Ryu, C. Y.; Benicewicz, B. C. *Macromolecules* **2006**, *39* (9), 3175−3183.
(19) Li, Y.; Benicewicz, B. C. *Macromolecules* **2008**, *41* (21), 7986−7992.
(20) Pryamtisyn, V.; Ganesan, V.; Panagiotopoulos, A. Z.; Liu, H. J.; Kumar, S. K. *J. Chem. Phys.* **2009**, *131* (22), 2221102−4.
(21) Bozorgui, B.; Meng, D.; Kumar, S. K.; Chakravarty, C.; Cacciuto, A. *Nano Lett.* **2013**, *13* (6), 2732−2737.
(22) Lu, P. J.; Zaccarelli, E.; Ciulla, F.; Schofield, A. B.; Sciortino, F.; Weitz, D. A. *Nature* **2008**, *453* (7194), 499−U4.
(23) Stradner, A.; Sedgwick, H.; Cardinaux, F.; Poon, W. C. K.; Egelhaaf, S. U.; Schurtenberger, P. *Nature* **2004**, *432* (7016), 492−495.
(24) Eberle, A. P. R.; Wagner, N. J.; Castaneda-Priego, R. *Phys. Rev. Lett.* **2011**, *106* (10), 105704.
(25) Michele, J.; Pätzold, R.; Donis, R. *Rheol. Acta* **1977**, *16* (3), 317−321.
(26) Pasquino, R.; Snijkers, F.; Grizzuti, N.; Vermant, J. *Rheol. Acta* **2010**, *49* (10), 993−1001.
(27) Scirocco, R.; Vermant, J.; Mewis, J. *J. Non-Newtonian Fluid Mech.* **2004**, *117* (2−3), 183−192.
(28) Won, D.; Kim, C. *J. Non-Newtonian Fluid Mech.* **2004**, *117* (2−3), 141−146.
(29) Leal, L. G. *J. Non-Newtonian Fluid Mech.* **1979**, *5* (0), 33−78.
(30) Snijkers, F.; Vlassopoulos, D. *J. Rheol.* **2011**, *55* (6), 1167−1186.
(31) Meissner, J.; Garbella, R. W.; Hostettler, J. *J. Rheol.* **1989**, *33* (6), 843−864.
(32) Schweizer, T. *J. Rheol.* **2003**, *47* (4), 1071−1085.
(33) Ilavsky, J.; Jemian, P. R.; Allen, A. J.; Zhang, F.; Levine, L. E.; Long, G. G. *J. Appl. Crystallogr.* **2009**, *42* (3), 469−479.
(34) Beaucage, G. *J. Appl. Crystallogr.* **1996**, *29* (2), 134−146.
(35) Moll, J. F.; Akcora, P.; Rungta, A.; Gong, S. S.; Colby, R. H.; Benicewicz, B. C.; Kumar, S. K. *Macromolecules* **2011**, *44* (18), 7473−7477.
(36) Koumakis, N.; Petekidis, G. *Soft Matter* **2011**, *7* (6), 2456−2470.
(37) Pham, K. N.; Petekidis, G.; Vlassopoulos, D.; Egelhaaf, S. U.; Poon, W. C. K.; Pusey, P. N. *J. Rheol.* **2008**, *52* (2), 649−676.
(38) Shih, W. H.; Shih, W. Y.; Kim, S. I.; Liu, J.; Aksay, I. A. *Phys. Rev. A* **1990**, *42* (8), 4772−4779.
(39) Mobuchon, C.; Carreau, P. J.; Heuzey, M.-C. *J. Rheol.* **2009**, *53* (3), 22.
(40) Mohraz, A.; Solomon, M. J. *J. Rheol.* **2005**, *49* (3), 25.
(41) Masschaele, K.; Vermant, J. *J. Rheol.* **2009**, *53* (6), 24.
(42) Rajaram, B.; Mohraz, A. *Soft Matter* **2010**, *6* (10), 2246−2259.
(43) Rajaram, B.; Mohraz, A. *Phys. Rev. E* **2011**, *84* (1), 011405.
(44) Kumar, S. K.; Jouault, N.; Benicewicz, B.; Neely, T. *Macromolecules* **2013**, *46* (9), 3199−3214.
(45) Masschaele, K.; Fransaer, J.; Vermant, J. *J. Rheol.* **2009**, *53* (6), 1437−1460.
(46) Pignon, F.; Magnin, A.; Piau, J. M. *Phys. Rev. Lett.* **1997**, *79* (23), 4689−4692.
(47) Wilking, J. N.; Chang, C. B.; Fryd, M. M.; Porcar, L.; Mason, T. G. *Langmuir* **2011**, *27* (9), 5204−5210.
(48) Koppi, K. A.; Tirrell, M.; Bates, F. S.; Almdal, K.; Colby, R. H. *J. Phys. II* **1992**, *2* (11), 1941−1959.